

## Research Article

# Comparison and Analysis of the Performances and Mechanisms of Recycled Asphalt Incorporating High-Permeability Rejuvenating Agent

Yanjuan Tian,<sup>1</sup> Mulian Zheng ,<sup>1</sup> Hailei Xu,<sup>2</sup> Chupeng Chen,<sup>1</sup> and Jinhao Zhang<sup>1</sup>

<sup>1</sup>Key Laboratory for Special Area Highway Engineering of Ministry of Education, Chang'an University, South Erhuan Middle Section, Xi'an 710064, Shaanxi, China

<sup>2</sup>Highway Administration Bureau of Xiuzhou District, Jiaxing City 314000, Zhejiang, China

Correspondence should be addressed to Mulian Zheng; zhengml@chd.edu.cn

Received 15 April 2019; Revised 13 July 2019; Accepted 21 July 2019; Published 20 August 2019

Academic Editor: Yuqing Zhang

Copyright © 2019 Yanjuan Tian et al. This is an open access article distributed under the Creative Commons Attribution License, which permits unrestricted use, distribution, and reproduction in any medium, provided the original work is properly cited.

The objective of this study is to develop a highly permeable rejuvenating agent for the recycling of the asphalt pavement. The rheological properties and permeability of recycled asphalt after adding the self-developed rejuvenating agent, as well as two other agents, were compared and evaluated. An improved softening point method was devised to evaluate the permeability. In addition, the recycled asphalt was analyzed using Fourier transform infrared spectroscopy (FTIR). The results showed that the self-developed rejuvenating agent had high permeability, could effectively restore the performance of the aged asphalt, and could improve the aging-resistant property of the recycled asphalt. FTIR analysis showed that the matrix asphalt experienced oxygen absorption and dehydrogenation during the aging process. The aging of the SBS-modified asphalt was achieved via dual aging of the matrix asphalt and SBS-modified components. In addition, the rejuvenating agent CA had an inhibitory effect on asphalt aging, and its recycling efficiency was better than that of the rejuvenating agent A for the aged SBS-modified asphalt. Finally, a relationship between the microscopic functional group index and the macroscopic test index was established.

## 1. Introduction

Currently, the circular economy and green economy are being vigorously promoted during development of the world. The recycling of waste asphalt mixtures has attracted more and more attention because it is beneficial to environmental protection. Rejuvenating agents are used for recycling waste asphalt mixtures. Rejuvenating agents with good properties could be compatible with aged asphalt to improve its performance, thus extending the service life of the pavement [1–4]. From their initial application during the oil crisis stage to popularization in the United States in the late 1980s, reclaimed asphalt mixtures have been greatly utilized with the development of rejuvenating agents, with a use ratio greater than 80%. The development of rejuvenating agents continues all over the world, and their technical indicators and evaluation methods are continuously

studied. Rejuvenating agents should have excellent permeability and should fully mix the aged asphalt in order to effectively restore the performance and structure of the aged asphalt.

Carpenter and Wolosick [5] illustrated that rejuvenating agents with low viscosity have a great influence on diffusion capability and can be quickly mixed with the aged asphalt to reach the required viscosity and effectively restore its performance. Cussler [6] and Karlsson and Isacsson [7] investigated the diffusion process of the rejuvenating agents, as demonstrated through the marker using FTIR technology. Yu and Zheng [8] studied the influence of the diffusion temperature and the viscosity of rejuvenating agents on the diffusion law according to the crack diffusion model and presented a method that increased the diffusion coefficient and amount. Karlsson and Isacsson [7, 9] analyzed rejuvenating agent diffusion via its methyl and carbonyl

contents using FTIR. Wang et al. [10] investigated the recycling effects and diffusion properties using static penetration tests and proposed that the concentration difference and macromolecular blocking were significant influencers on the penetration effect. Sun et al. [11] proposed that the aging of SBS-modified asphalt included matrix asphalt and SBS aging, and adding a rejuvenating agent could increase the recovery efficiency under the conditions of an appropriate mixing temperature and time. Ma et al. [12] suggested that low-viscosity rejuvenating agents could raise the diffusion efficiency but that the thermal stability was poor. In addition, they noted that the performance of the recycled asphalt may be adversely affected if different components of the rejuvenating agents cannot simultaneously diffuse into the aged asphalt. Zhang [13] investigated the influence of the rejuvenating agent content on the properties of hot, recycled asphalt mixtures with high proportions of the reclaimed asphalt pavement (RAP). He suggested that a too low proportion of a rejuvenating agent may cause a significant reduction in the water stability of the recycled asphalt and, in contrast, may affect performance at high temperature. A total of 8% was determined as the optimum blending ratio of the rejuvenating agents. Ran et al. [14] studied SBS-modified rejuvenating agents. They identified the composition of rejuvenating agent swelling solutions via orthogonal tests, analyzed their recycling effect by FTIR, and evaluated high- and low-temperature properties via the dynamic shear rheological (DSR) tests and bending beam rheometer (BBR) methods. Li et al. [15] analyzed the recycling mechanism of aged SBS-modified asphalt based on the cross-linking relationship between the matrix asphalt and the modified component. Xu et al. [16] established molecular dynamic models of aged asphalt to investigate the diffusion mechanism of the rejuvenating agent. They found that molecular force contributed to the diffusion of the rejuvenating agent and asphalt. Mohamed et al. [17] studied the oxidative stability of the rejuvenating agent using thermogravimetric analysis (TGA) and observed its crystallization and melting points using differential scanning calorimetry (DSC). Zhang et al. [18] used bio-oil generated from sawdust as a rejuvenator to the reclaimed asphalt pavement. They applied the rotational viscometer (RV) test, FTIR, and DSR test to characterize the properties of rejuvenated asphalt. They found that the sulfoxide index and aromatic index could be used to assess the performances of the recycled asphalt, but carbonyl was not applicable. Haghshenas et al. [19] investigated two rejuvenating agents including a petroleum-tech (aromatic extracts) and a green-tech (tall oil) by means of saturate-aromatic-resin-asphaltene (SARA) analysis, FTIR, TGA, and nuclear magnetic resonance (NMR). They indicated that the tall oil contained many hydrogen bond-forming -OH functional groups, which can increase the moisture sensitivity of the asphalt mixture, while the aromatic extracts without the -OH functional groups did not show such a high moisture susceptibility. Caputo et al. [20] assessed the structure of two biocompatible rejuvenating agents using powder X-ray diffraction (PXRD) measurements and NMR and their chemical action when added to asphalt.

Most studies have focused on restoring a certain property of aged asphalt, the recycling effect, the mechanism, and the diffusion mechanism of rejuvenating agents, while fewer studies have investigated rejuvenating agents with high permeability. Meanwhile, numerous studies have investigated the macroperformances and microstructures of recycled asphalt, but the correlation between them has rarely been studied.

This research aimed to develop a highly permeable rejuvenating agent for asphalt pavement recycling. A rejuvenating agent was developed, and the rheological properties and permeability of the recycled asphalt after adding the agent were systematically investigated. The recycling mechanism was analyzed via FTIR. Two other rejuvenating agents were also used for comparison. The self-developed rejuvenating agent had high permeability, had an inhibitory effect on asphalt aging, and effectively restored the properties of aging asphalt. Finally, the recycling mechanism of recycled asphalt was qualitatively and quantitatively analyzed by FTIR, and a relationship between the microscopic functional group index and macroscopic test indicators was established to further reveal the recycling mechanism of the aged asphalt.

## 2. Materials and Experiments

*2.1. Raw Materials.* A highly permeable rejuvenating agent (CA) was developed for the hot recycling of the asphalt pavement in this study. Based on the concepts of adding missing components, repairing the aging structure, and improving permeability, our research team developed CA. The raw materials of CA are composed of base oil, a plasticizer, an antiager, a structure-repairing agent, and a penetrant, as listed in Table 1. The base oil is obtained via the catalytic cracking of crude oil and has a low acidity value and a high aromatic content, especially saturated hydrocarbons and monocyclic and bicyclic aromatic hydrocarbons. Because of the lower viscosity, it can be compatible with aged asphalt. It is used to blend the components of asphalt, change the heavy qualitative reaction of aged asphalt, and increase active substances. The polar groups in the plasticizer will interact with those in the aged asphalt, weakening the attraction between the asphalt molecules and reducing the entanglement of molecular chains. Therefore, the aged asphalt becomes more flexible, improving its performance. The antiager has a strong antioxidation ability, good stability, high temperature resistance, and lower price. It can effectively prevent the heating and oxidative aging of asphalt and increase the antiaging properties of recycled asphalt. The structure-repairing agent is selected from a glycerol ether compound. It contains chemical groups to repair some broken chains of the aged asphalt or to modify the asphalt to improve its performance. The penetrant is a nonionic surfactant, which has excellent wetting and permeating properties.

Because of adding the accelerating permeation component (Penetrant J) to CA, the mixing time and energy consumption in the mixing process are reduced, which makes it more environmentally friendly. Furthermore, CA

TABLE 1: Raw materials and dosages of CA.

Ingredient	Proportion (%)
Base oil X	76.64
Plasticizer Y	11.21
Antiager Z	5.61
Structure-repairing agent K	5.61
Penetrant J	0.93

merges with aging asphalt more quickly to form new asphalt structures in the mixing process, resulting in less volatile substances under the accelerated heating in the course of the mixing processes and field aging. The aromatic hydrocarbons in CA exist in the form of new asphalt components, so its thermal stability is greatly improved, which is close to the thermal stability of the components of original asphalt. Meanwhile, in the current laboratory research stage, the use of CA in recycling asphalt imposed less additional burden on the environment.

The other two rejuvenating agents included RA-100 (A) produced by Jiangsu and an ordinary rejuvenating agent (B) produced by Guangdong. #70 matrix asphalt and SBS-modified asphalt I-C were used in this study. The parameters of the matrix asphalt and SBS-modified asphalt are listed in Table 2.

## 2.2. Experiments

**2.2.1. Routine Tests.** The extracted aged asphalt from the reclaimed asphalt pavement is generally impure, as it contains mineral powder and volatile trichloroethylene. Therefore, this approach cannot truly present the performance of actual aged asphalt, and it has a lower extraction efficiency. Considering the limitations of the extraction method, aged asphalt samples were prepared using the rotating thin film oven test (RTFOT) [22] in this study. Huang et al. [23] suggested that the RTFOT could simulate the aging of the actual asphalt pavement. Li found that [24] the aging test RTFOT (270 min) has approximately the same effect as the pressurized aging vessel (PAV) test. Therefore, the RTFOT (5 h) asphalt sample was used to simulate the asphalt aging in the actual pavement to study the restoring performance of the rejuvenator in this study. CA, A, and B were added to the aged matrix asphalt and SBS-modified asphalt. According to Chen's previous research [25], the rejuvenating agent was mixed with asphalt with a proportion of 7 wt.%, at which the recycled asphalt has a good effect. The penetration, softening point, viscosity, and ductility of the recycled asphalt were tested in this section according to the current specification of China [21].

**2.2.2. Rheological Properties of the Recycled Asphalt.** Dynamic rheological properties, which are chief indicators for evaluating asphalt pavement performance in the Strategic Highway Research Program (SHRP), are measured by DSR. The complex shear modulus ( $G^*$ ) and phase angle ( $\delta$ ) are measured to characterize the viscosity and elasticity of

the asphalt binder, respectively. The rutting factor ( $G^*/\sin \delta$ ) is used to evaluate the rutting resistance of the asphalt pavement at high temperature.

The Anton Paar MCR 102 advanced rheometer was used for DSR tests. The shear strain control mode was applied in the tests. DSR tests were conducted to measure  $G^*$ ,  $\delta$ , and  $G^*/\sin(\delta)$  of the samples. The samples included the eight groups that are listed in Table 3.

**2.2.3. Permeability of Recycled Asphalt.** The penetration and softening point methods are common methods for evaluating the macroscopic properties of recycled asphalt. The former is widely applied in testing the permeability of rejuvenating agents, but the latter is used less frequently. In this study, these two test methods were used to evaluate the permeability of the rejuvenating agents.

**(1) Penetration Method.** The aged matrix asphalt and aged SBS-modified asphalt were placed into the penetration test molds to prepare three samples. Then, CA, A, and B were applied evenly to the surfaces of the samples (the aged asphalt). The samples were placed in a 135°C oven for 30 min. The penetration of the samples was tested every 5 min, for which three values were measured for each sample and the average value was taken as the result.

**(2) Improved Softening Point Method.** The above penetration method is commonly performed under room temperature conditions. The method presented in this study, the improved softening point method, is used to evaluate the permeable performance under high-temperature conditions. As shown in Figure 1, the four softening point test molds are stacked together and numbered H1, H2, H3, and H4 from top to bottom. Plasticine was used to fill the gaps between molds to prevent the upper, convex portion of the mold from affecting the molding. The prepared aged asphalt was poured into the test molds, and then the rejuvenating agents were painted on the uppermost layers. Subsequently, the test molds were placed in a 135°C oven for 10 min. For heating time, four groups of time (5 min, 10 min, 15 min, and 20 min) were chosen to conduct trial tests. The results indicated that heating for 5 min was too short, and the rejuvenating agent could not penetrate to the bottom of the four samples. After heating for more than 15 minutes, the softening points of the four specimens remained consistent, indicating that the rejuvenating agent had evenly penetrated into the four samples. In order to study the change of permeability, it was reasonable to choose 10 min as the heating time. For heating temperature, 135°C was chosen in this study. According to the current specification of China [26], for #70 asphalt, its heating time is 155~165°C, the discharge temperature of the asphalt mixture is 145~165°C, and the paving temperature of its mixture shall not be lower than 135°C. Therefore, 155°C, 145°C, and 135°C were selected for trial tests, and it was found that the permeating rate was too fast for observing the penetration law at 155°C and 145°C, so 135°C was determined as the heating temperature in this study.

TABLE 2: Main indicators of the matrix asphalt and SBS-modified asphalt.

Parameters	Matrix asphalt	SBS-modified asphalt I-C	Normative value	Measurements <sup>1</sup>
Penetration (25°C, 100 g, 5 s) (dmm)	66.7	67.2	60–80	T0604
Ductility (5 cm/min) (cm)	>100	34.5	≥100	T0605
Softening point (ring and ball) (°C)	46.7	62.7	≥43	T0606
Viscosity (135°C) (mPa·s)	257.8	3100	—	T0625

<sup>1</sup>The test methods described are provided in reference [21].

TABLE 3: Matrix asphalt and SBS-modified asphalt samples.

Samples	Asphalt types
1	Original matrix asphalt
2	Aged matrix asphalt via RTFOT
3	Original SBS-modified asphalt
4	Aged SBS-modified asphalt via RTFOT
5	Aged matrix asphalt + CA (7 wt.%)
6	Aged matrix asphalt + A (7 wt.%)
7	Aged SBS-modified asphalt via RTFOT + CA (7 wt.%)
8	Aged SBS-modified asphalt via RTFOT + A (7 wt.%)



FIGURE 1: Test molds of the improved softening point method.

After cooling at room temperature, the residual plasticine on the test molds was scraped off and the molds were cut with a thin blade. Finally, the softening point of each sample was measured at three points, and the average value was taken as the result. In this study, H1, H2, H3, and H4 are assumed to be different penetration depths h1, h2, h3, and h4, respectively, and the softening point of each mold corresponds to that of different depths.

#### 2.2.4. Fourier Transform Infrared Spectroscopy (FTIR).

The contents of special functional groups in aged asphalt, such as carbonyl and sulfoxide groups, can be quantitatively analyzed by characteristic absorption peaks using Fourier transform infrared spectroscopy. The diffusion effect among the original asphalt, rejuvenating agents, and aged asphalt can also be investigated via FTIR-ATR [27–31]. The samples included eight groups: matrix asphalt, aged matrix asphalt, SBS-modified asphalt, aged SBS-modified asphalt, aged matrix asphalt after adding CA, aged matrix asphalt after adding A, aged SBS-modified asphalt after adding CA, and aged SBS-modified asphalt after adding A. Among them, the amount of the rejuvenating agent is 7% of the mass of the asphalt. Each sample was dissolved in carbon disulfide with a mass concentration of 5%. One drop of the solution was dropped on the potassium

bromide wafer, and the FTIR test was conducted after the carbon disulfide was completely volatilized. The Cary 600 Series FTIR spectrometer manufactured by Agilent Technologies was used for infrared analysis in this study. The scanning range was  $400\text{ cm}^{-1}$  to  $4000\text{ cm}^{-1}$ , the resolution was  $4\text{ cm}^{-1}$ , the signal-to-noise ratio was 40000:1, and the number of scans was 32 times. Infrared spectroscopy was performed by Thermo Scientific OMNIC™ 8.2 software [32]. OMNIC, the professional infrared analysis software developed by Nicolet, can perform qualitative and quantitative analyses of spectral images.

Recent studies have shown that the degrees of aging and recycling of asphalt can be assessed by the specific gravity of the functional groups. An aliphatic functional group index (BI), an aromatic functional group index (AI), a hydroxyl functional group index (CI), and a sulfoxide functional group index (DI) were introduced to quantitatively analyze aging and recycling phenomena by calculating the areas of the relevant functional groups. The four functional groups represent the long-chain alkyl group, the benzene ring substitute, and the asphalt aging product content, respectively. The relevant calculations are expressed as formulas (1)–(4):

$$BI = \frac{A_{1456\text{ cm}^{-1}\text{-CH}} + A_{1376\text{ cm}^{-1}\text{-CH}_3}}{\sum A}, \quad (1)$$

$$AI = \frac{A_{1600\text{ cm}^{-1}\text{C=C}}}{\sum A}, \quad (2)$$

$$CI = \frac{A_{1730\text{ cm}^{-1}\text{C=O}}}{\sum A} \quad (3)$$

$$DI = \frac{A_{1030\text{ cm}^{-1}\text{S=O}}}{\sum A}, \quad (4)$$

where  $\sum A$  denotes the peak area of the sample.

As shown in Figure 2, the area of the functional groups for different samples at  $X\text{ cm}^{-1}$  is defined as the area enclosed by the tangent line and the curve on both sides of the indicated  $X\text{ cm}^{-1}$ .

### 3. Results and Discussion

3.1. Results and Analysis of Routine Tests. The measured penetration, viscosity, ductility, and softening point of the samples are shown in Figures 3–6, where a, b, c, d, and e, respectively, denote the samples of aged asphalt, original asphalt, aged asphalt with added rejuvenating agent CA,

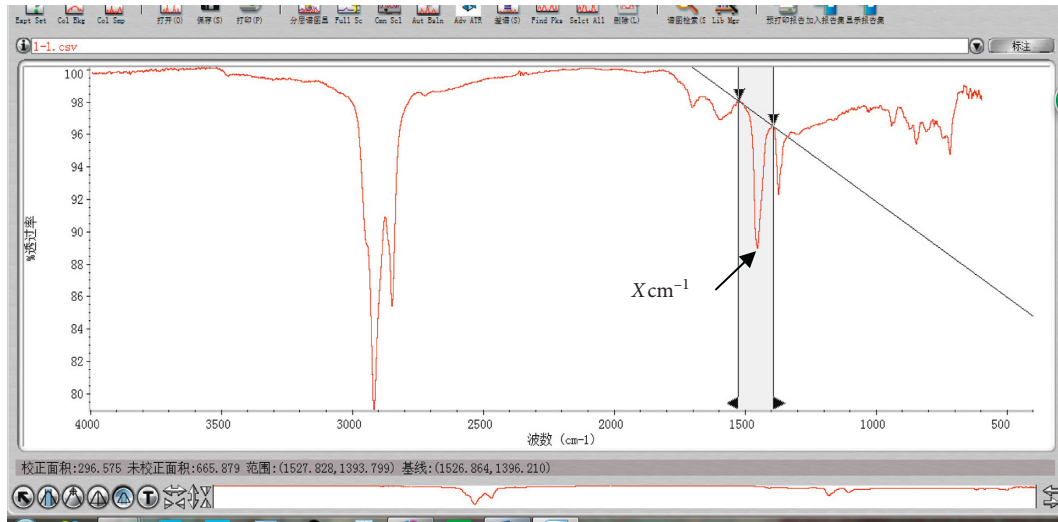


FIGURE 2: Schematic diagram of the functional group area at  $X\text{ cm}^{-1}$ .

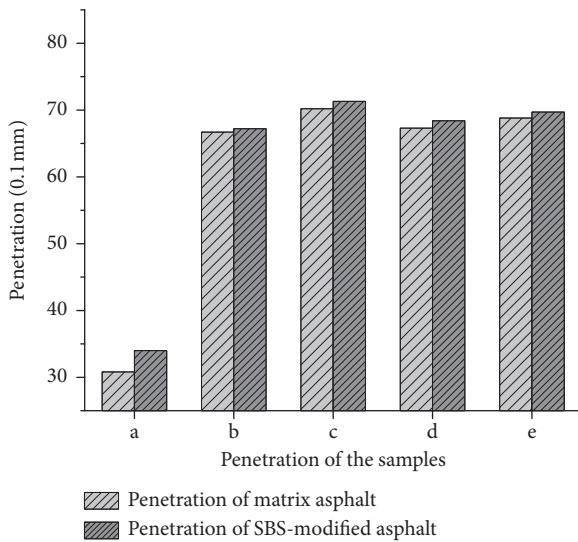


FIGURE 3: Penetration of the samples.

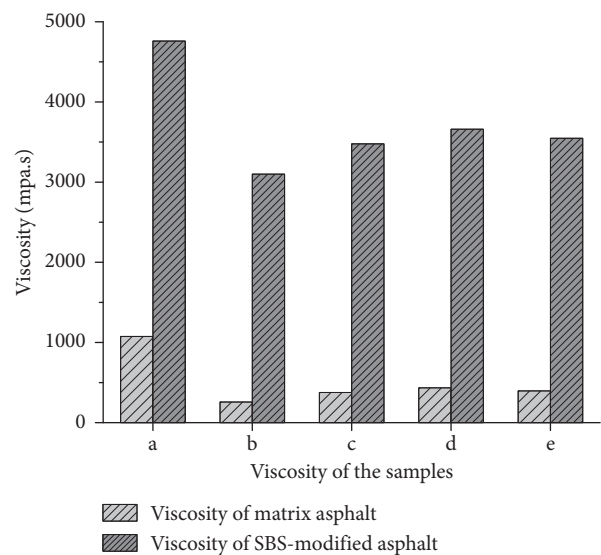


FIGURE 4: Viscosity of the samples.

aged asphalt with added rejuvenating agent B, and aged asphalt with added rejuvenating agent A.

As shown in Figures 3–6, the results indicated that the performances of the recycled asphalt can be recovered effectively, meeting the requirements of the specification after adding the rejuvenating agents. However, the effects of different rejuvenating agents in restoring the aged asphalt are different. Compared to B and A, CA had a better performance in the recycling effect on aged asphalt; the performance of recycled asphalt treated with CA was closest to that of the original asphalt and was even somewhat better.

**3.2. Results and Discussion of the DSR Tests.** The results of  $G^*$ ,  $G^*/\sin \delta$ , and  $\delta$  measured by DSR tests are, respectively, shown in Figures 7–9.

As shown in Figure 7, for both matrix asphalt and SBS-modified asphalt,  $G^*$  increased significantly after aging, but

it decreased significantly after adding rejuvenating agents. Both Figures 7(a) and 7(b) show that the  $G^*$  decreased sharply after incorporating CA and that the  $G^*$  of the recycled matrix asphalt is lower than that of the original asphalt, while it is the same as that of the recycled SBS-modified asphalt. The curves after incorporating CA are at the bottom and indicate that CA could lower the viscosity of the aged asphalt. This may be due to the large percentage of base oil in CA.

Figure 8 shows variation in the rutting factor ( $G^*/\sin \delta$ ) before and after asphalt recycling.  $G^*/\sin \delta$  increases significantly after aging and decreases after rejuvenating agents are incorporated. Especially after incorporating CA, it is shown in both Figures 8(a) and 8(b) that  $G^*/\sin \delta$  decreases significantly. The rutting factor of the recycled asphalt that incorporates CA is higher than that of original asphalt at high temperature, indicating that it has superior rutting

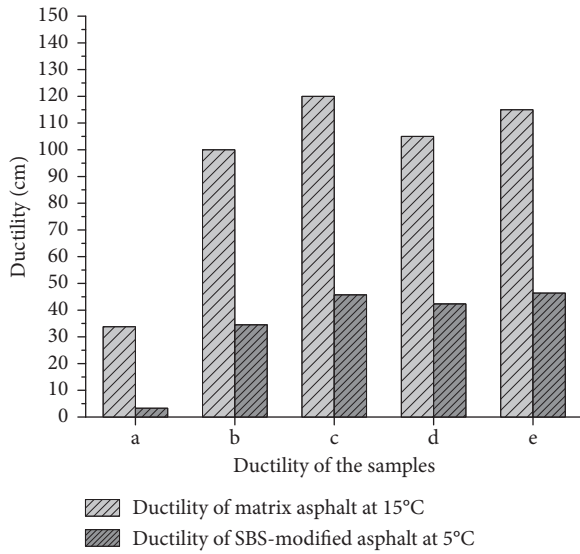


FIGURE 5: Ductility of the samples.

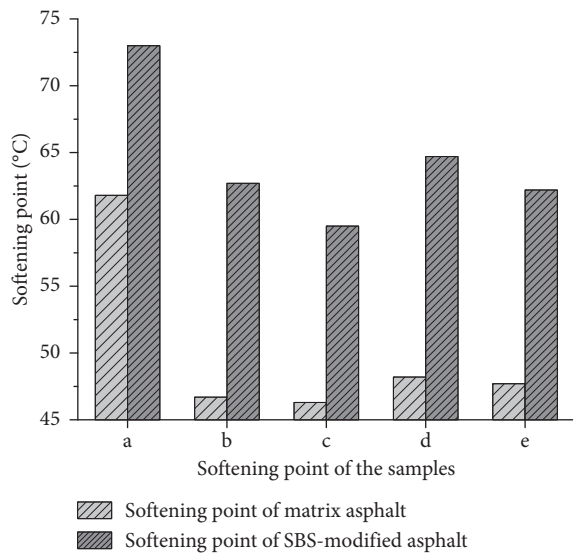
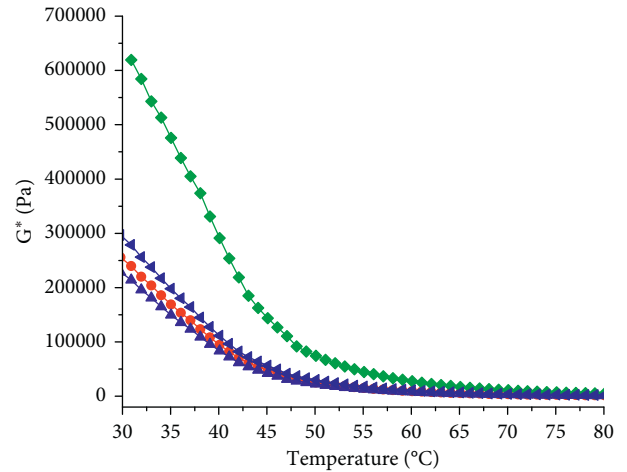


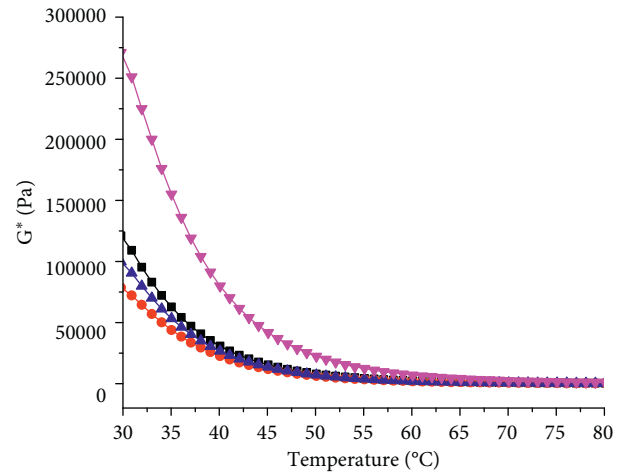
FIGURE 6: Softening point of the samples.

resistance. Nevertheless, the rutting resistance of the recycled asphalt mixture at high temperature is also a topic of further study for the research plan.

As shown in Figure 9, the phase angles ( $\delta$ ) of both asphalt samples decrease after aging and increase somewhat after recycling. The  $\delta$  values of the recycled SBS-modified asphalt varied greatly: at low temperature (less than 50°C), they were lower than those of the original asphalt, and as the temperature increased (greater than 50°C), their growth rate was faster, even greater than that of original asphalt. This may be related to the aged SBS-modified component. The asphalt consistency is higher at lower temperatures, and  $\delta$  is small. The rejuvenating agents supplemented the lost light component of the aged asphalt, leading to an increase in fluidity of the recycled asphalt and a significant increase in the rate of  $\delta$ , especially at temperatures higher than 50°C. CA has a



(a)



(b)

FIGURE 7:  $G^*$  variation before and after asphalt recycling: (a) SBS-modified asphalt; (b) matrix asphalt.

similar effect to that of A, with the results of CA closest to those of the original asphalt.

### 3.3. Analysis of the Permeability Test Results

3.3.1. Results of the Penetration Method. Penetration values were tested after adding different rejuvenating agents to aged asphalt samples. The results are shown in Figure 10.

As shown in Figure 10, the change in penetration can be simply divided into three stages: an initial stage of rapid penetration, an intermediate stage of slow penetration, and a final stage of stability. The six samples were basically within

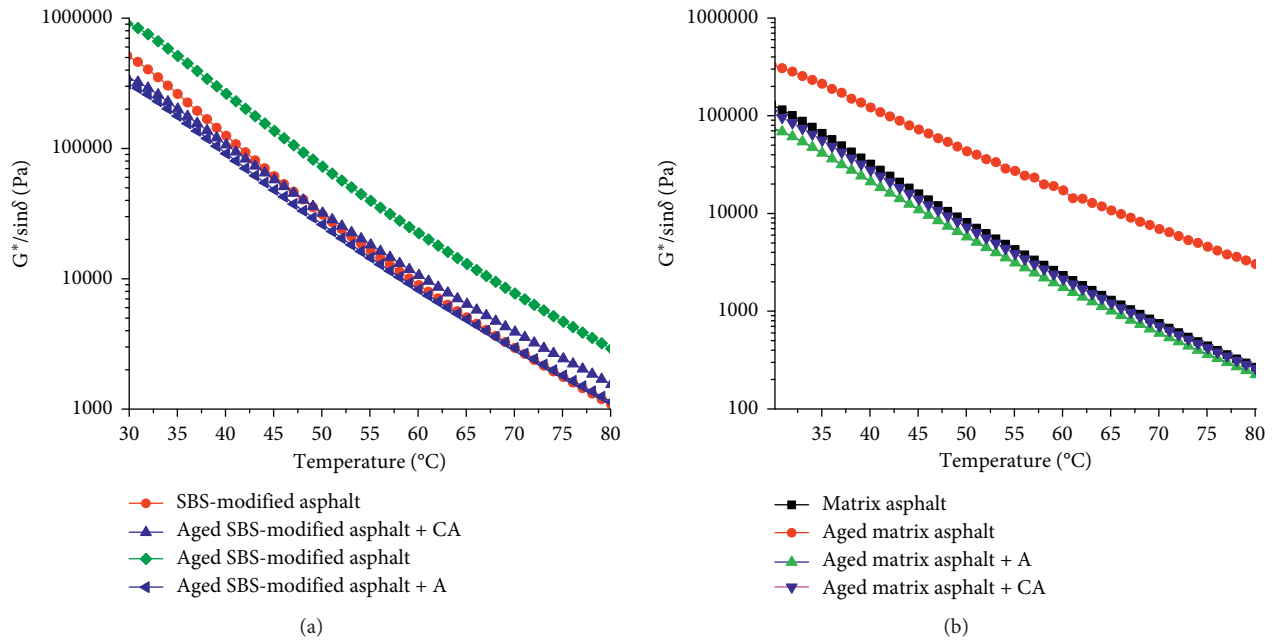


FIGURE 8: Variation in  $G^*/\sin \delta$  before and after asphalt recycling: (a) SBS-modified asphalt; (b) matrix asphalt.

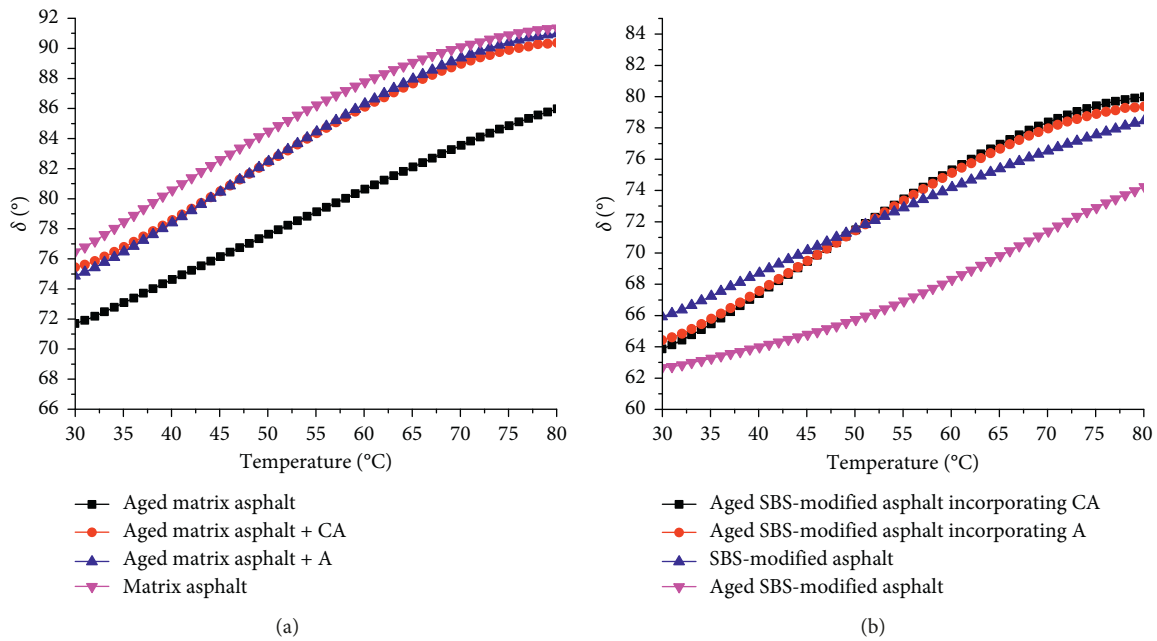


FIGURE 9:  $\delta$  curves of asphalt at different temperatures: (a) matrix asphalt and (b) SBS-modified asphalt before and after recycling.

the rapid penetration stage from 0 to 5 min, and the penetration speeds of rejuvenating agents in the matrix asphalt were higher than that of SBS-modified asphalt. The slow penetration occurred from 5 to 15 min, which was the development period of the penetration. As the rejuvenating agents permeated through the upper layer to the lower layer, the rate gradually slowed. At this stage, the penetration of SBS-modified asphalt still increased gradually. However, the growth was extremely limited, and the matrix asphalt instead showed a slight decreasing trend. This result may be due to

the slight aging of the recycled asphalt on the surface of the mold.

The curves in Figure 10 were fitted with the penetration and temperature logarithms. The formulas are listed in Table 4. The results indicate that the penetration and temperature logarithms are well correlated, with correlation coefficients greater than 0.9. Comparing the regression coefficients of the three rejuvenating agents, the permeability of CA is greater than that of A and B. CA exhibits superior high permeability in both the rapid penetration and intermediate

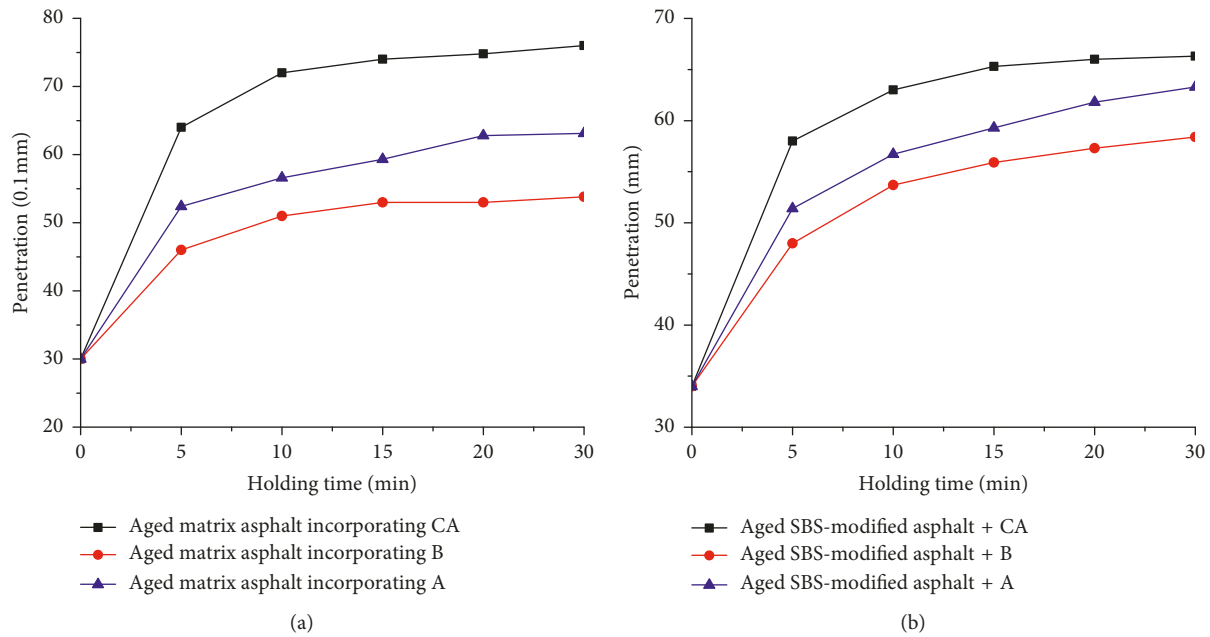


FIGURE 10: Penetration curves of aged asphalt after adding rejuvenating agents at a certain holding time: (a) recycled matrix asphalt; (b) recycled SBS-modified asphalt.

TABLE 4: Change curves of penetration of two regenerated asphalt samples.

Asphalt type	Rejuvenating agents	Fitting formula	$R^2$
Aged SBS-modified asphalt	B	$P = 19.092 \lg t + 35.112$	0.9795
	A	$P = 20.175 \lg t + 35.408$	0.9822
	CA	$P = 22.481 \lg t + 37.585$	0.9157
Aged matrix asphalt	B	$P = 16.682 \lg t + 32.082$	0.9399
	A	$P = 22.832 \lg t + 32.521$	0.9567
	CA	$P = 31.785 \lg t + 35.185$	0.912

stages. The curves do not cross in Figures 10(a) and 10(b), showing that accelerated infiltration will not occur during infiltration. Thus, the permeability of the rejuvenating agent as evaluated by the penetration method is reasonable.

**3.3.2. Results of the Improved Softening Point Method.** The permeability was studied by testing the softening points of samples after adding different rejuvenating agents. The test results are plotted in Figure 11.

Permeability curves featuring the improved softening point method are shown in Figure 11. The permeability of CA is greater than that of A and B, which is consistent with the conclusion obtained by the penetration method. It could be considered that CA has excellent permeability and can penetrate into the interior of the aged asphalt more quickly under the same conditions to improve the performance of aged asphalt. From the curves in Figure 11, it can be seen that the softening point at h1 is similar to that of the recycled asphalt, that at h2 has a significant recovery, and after h3, there are insignificant changes. This result may be related to the test setting temperature and holding time such that the penetration depth of the rejuvenating agents is not reached. From the fitting formulas listed in Table 5, it can be seen that

the improved softening point method is feasible to evaluate the permeability. In addition, the permeability of CA is greater according to the comparison of correlation coefficients.

### 3.4. FTIR Results

**3.4.1. Qualitative Analysis.** Figure 12 shows the infrared spectrogram of the aged and unaged matrix asphalt. The stretching vibration of saturated hydrocarbon and its derivatives, C-H and  $-\text{CH}_2$ , was less than  $3000 \text{ cm}^{-1}$ , which was the dividing line between the saturated hydrocarbon and the unsaturated hydrocarbon; the absorption of  $-\text{CH}_2-$  was the strongest. The obvious absorption peaks at  $2920 \text{ cm}^{-1}$  and  $2850 \text{ cm}^{-1}$  could be used to determine saturated hydrocarbons in asphalt. The absorption peak at  $1600 \text{ cm}^{-1}$  was partly caused by the conjugate double bond C=C (benzene ring skeleton vibration) and partly caused by the absorption of C=O such that the existence of aromatic compounds could be determined. The two absorption peaks at  $1457 \text{ cm}^{-1}$  and  $1373 \text{ cm}^{-1}$ , respectively, represented the in-plane stretching vibrations of the functional groups C-CH and  $-\text{CH}_2-$ . According to the spectral analysis, the matrix asphalt

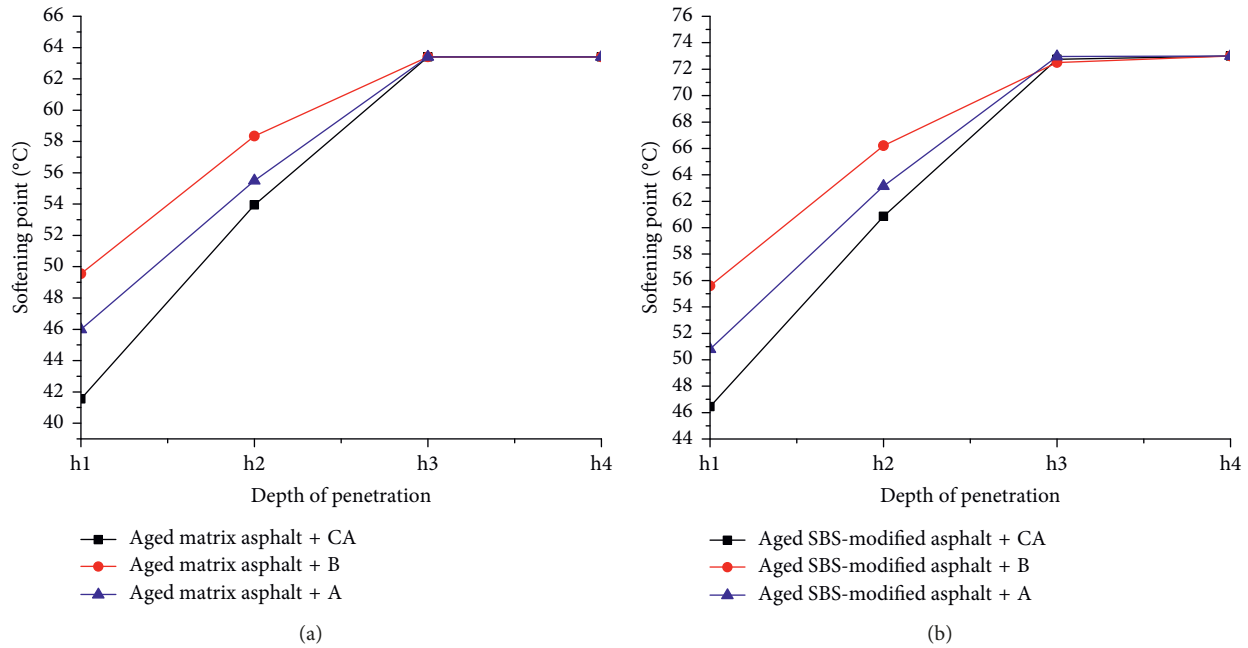


FIGURE 11: Softening point curves of aged asphalt after adding rejuvenating agents at a certain penetration depth: (a) recycled matrix asphalt; (b) recycled SBS-modified asphalt.

TABLE 5: Softening point fitting formulas.

Asphalt type	Rejuvenating agents	Fitting formula	$R^2$
Aged matrix asphalt	CA	$Y = 16.895 \ln X + 42.155$	0.9617
	B	$Y = 10.622 \ln X + 50.236$	0.9554
	A	$Y = 13.489 \ln X + 46.357$	0.9617
Aged SBS-modified asphalt	CA	$Y = 20.522 \ln X + 46.958$	0.9647
	B	$Y = 13.246 \ln X + 56.301$	0.967
	A	$Y = 17.175 \ln X + 51.329$	0.9626

was mainly composed of saturated hydrocarbons, aromatic compounds, and heteroatom derivatives.

After aging, the vibration peaks of the carbonyl group and the benzene ring skeleton at wavenumbers  $1640 \text{ cm}^{-1}$  and  $1456 \text{ cm}^{-1}$  showed slightly increased intensities, and the trends moved toward lower wavenumbers. The other peaks showed little change in intensity. However, the overall transmittance increased, indicating that the amount of saturated and aromatic hydrocarbons decreased and the aging of asphalt was obvious.

Figure 13 shows that the performance restored at the characteristic peaks was obvious after adding the rejuvenating agents, but it did not reach the level of the original asphalt. The rejuvenating agents supplemented the aged asphalt with light components, and their mechanism of action was mainly physical dispersion. New characteristic peaks appeared from  $960 \text{ cm}^{-1}$  to  $830 \text{ cm}^{-1}$ , which were related to the materials added to the rejuvenating agents. Rejuvenating agents CA and A had similar recovery effects on aged asphalt, aside from some nuances.

The infrared spectrogram of the SBS-modified asphalt is shown in Figure 14. Before aging, the characteristic peaks are similar to those of matrix asphalt, except in that

deformation, stretching, and skeleton vibrations are generated in the fingerprint area. After aging, the heights of the absorption peaks at  $2920 \text{ cm}^{-1}$  and  $2851 \text{ cm}^{-1}$  decreased. This finding indicated that the saturated hydrocarbon content decreased after aging. New characteristic peaks appeared at  $1732 \text{ cm}^{-1}$  and  $849 \text{ cm}^{-1}$ , representing an increase in aldehydes and ketones and the conversion of aromatics to colloids and asphaltenes. The  $\text{C}=\text{C}$  group corresponding to  $966 \text{ cm}^{-1}$  decreased obviously, and a carbonyl group, sulfoxide group, and  $\text{O}-\text{H}$  group appeared. This indicated that the aged SBS-modified asphalt included dual aging of the matrix asphalt and SBS-modified components and that its aging condition was also more serious.

As shown in Figure 15, after adding CA and A, the missing components of the aged asphalt were significantly supplemented, and the infrared spectrum curve was very close to that of the original asphalt. At wavenumbers  $2920 \text{ cm}^{-1}$ ,  $2850 \text{ cm}^{-1}$ ,  $1456 \text{ cm}^{-1}$ , and  $1375 \text{ cm}^{-1}$  in Figure 14, the heights of the characteristic peaks decreased, indicating that the CA supplemented the lost light components of the aged asphalt. Aging substances such as formaldehyde, ketone, carbonyl, and sulfoxide groups

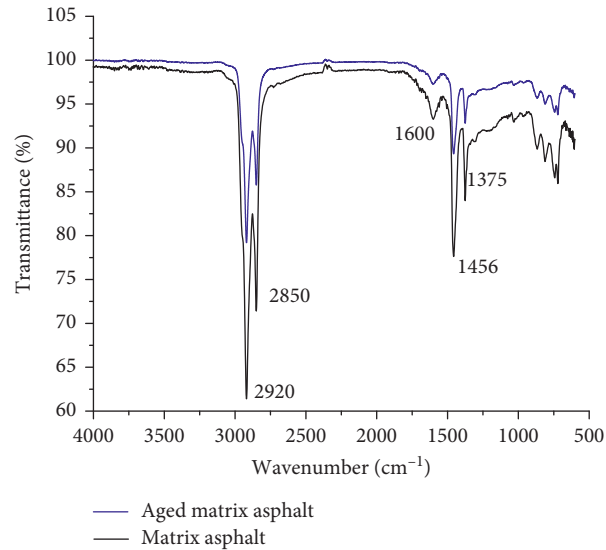


FIGURE 12: FTIR spectra of original and aged matrix asphalt.

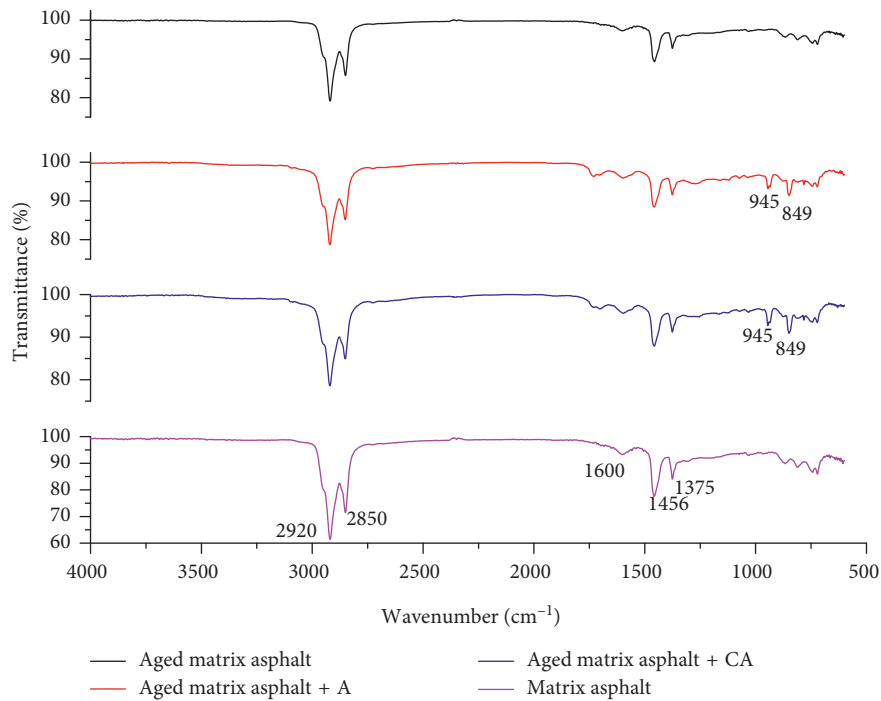


FIGURE 13: Comparison of FTIR spectra of several matrix asphalt samples.

were weakened at wavenumbers  $849\text{ cm}^{-1}$  and  $966\text{ cm}^{-1}$  shown in Figure 15, indicating that CA showed a reductive effect on these groups. It was concluded that CA had physical dispersion and chemical reduction effects on the aged SBS-modified asphalt and thus has antiaging properties.

**3.4.2. Quantitative Analysis.** If  $\sum A$  is chosen differently, the results vary widely when calculating the functional group indices. As such, the choice of  $\sum A$  requires a uniform standard. In this study, the C-H bond stretching vibration absorption peak

area at wavenumbers  $2920\text{ cm}^{-1}$  and  $2850\text{ cm}^{-1}$  was chosen as the reference, namely,  $\sum A = A_{2920\text{ cm}^{-1}} + A_{2850\text{ cm}^{-1}}$ . The results are shown in Table 6.

The BI represents the content of long-chain alkyl groups, the AI represents the content of benzene ring substituents, and the CI and DI, respectively, represent the contents of hydroxyl- and sulfoxide-based functional groups of asphalt aging products. As listed in Table 6, the CI and DI increased after aging and decreased after recycling, which was consistent with the results of the macroscopic performance and the recycling mechanisms.

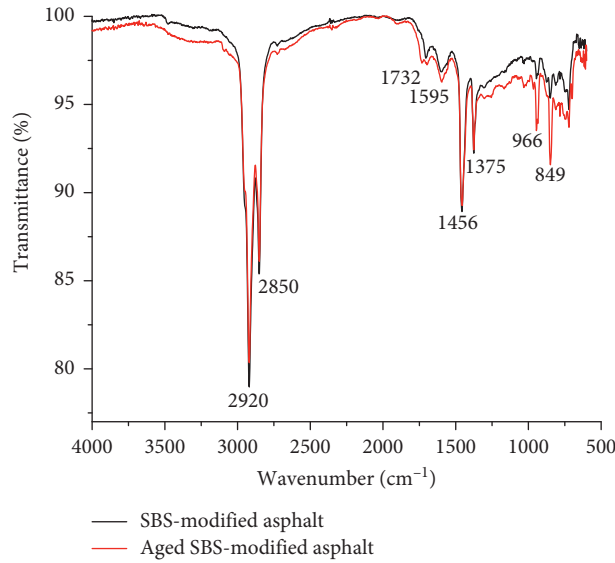


FIGURE 14: FTIR spectra of original and aged SBS-modified asphalt.

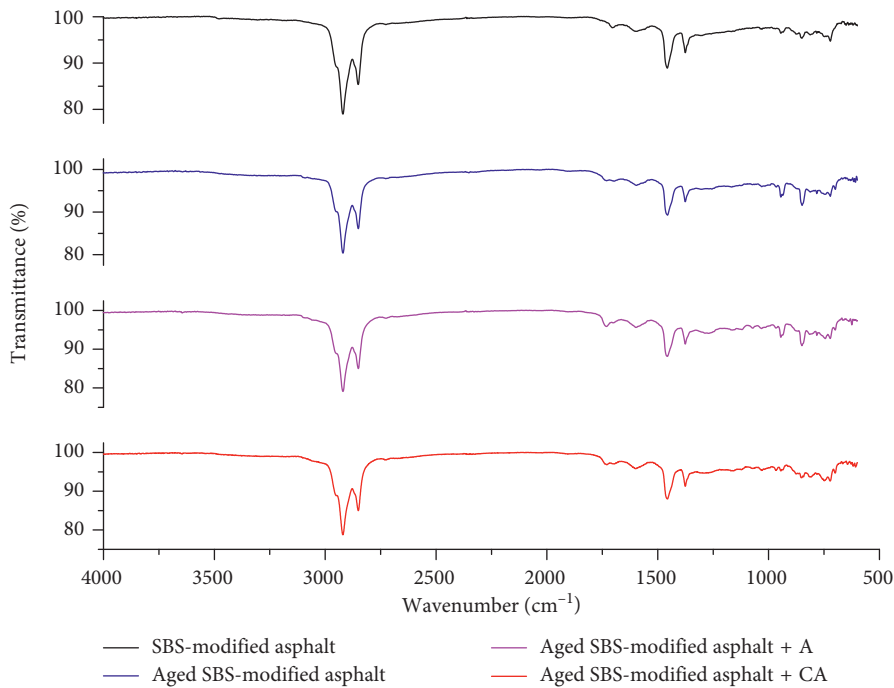


FIGURE 15: Comparison of FTIR spectra of several SBS-modified asphalt samples.

The four functional group indices of the two types of recycled asphalt were close to those of the original asphalt and were significantly different from those of the aged asphalt. This indicated that the composition and structure of the aged asphalt changed after recycling. For instance, the increase in the AI indicated that the light components in the recycled asphalt increased. Therefore, it may be conducive to investigating the recycling mechanism by establishing a relationship between the functional group index and the macroscopic indicator of the recycled

asphalt. According to Figures 5 through 8 and Table 6, the relationships between each functional group index and the three major indicators and viscosity of the recycled asphalt were established, as shown in Figures 16–19.

As shown in Figure 16, there is a good correlation between penetration and each functional group index. The penetration increased with the BI, decreased with the AI, and decreased with the CI and DI. The hydroxyl functional groups and sulfoxide functional groups represented by the CI and DI decreased to different degrees after incorporating

TABLE 6: Functional group indices for different states of asphalt.

Recycled asphalt	BI	AI	CI	DI
Matrix asphalt	0.2342	0.03654	0.0067	0.0038
Aged matrix asphalt	0.2243	0.04331	0.0983	0.0047
Recycled matrix asphalt + CA	0.2431	0.02534	0.00591	0.0037
Recycled matrix asphalt + A	0.2371	0.03893	0.00602	0.0035
SBS-modified asphalt	0.2401	0.04663	0.02361	0.0039
Aged SBS-modified asphalt	0.2324	0.05738	0.07907	0.0059
Recycled SBS-modified asphalt + CA	0.2548	0.04269	0.01334	0.0036
Recycled SBS-modified asphalt + A	0.2524	0.04476	0.03086	0.0035

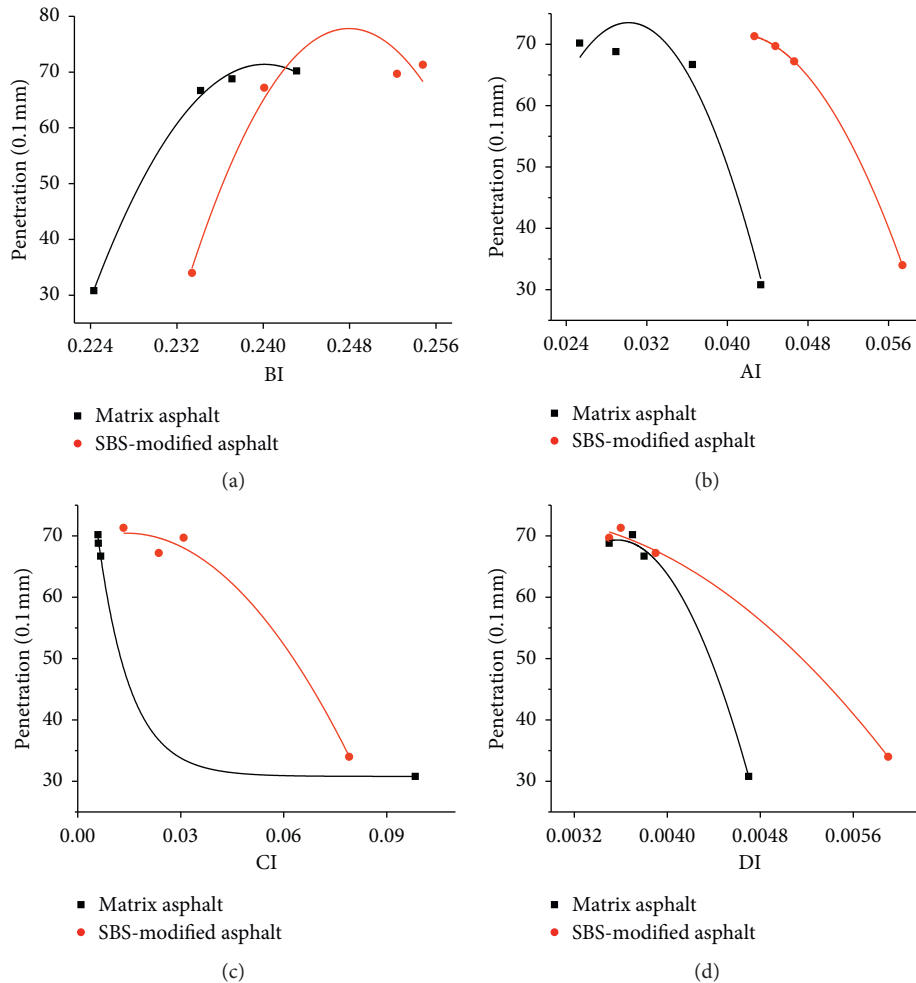


FIGURE 16: Relationships between the functional group indices and penetration.

different rejuvenating agents. C=O was reduced to C=C and S=O was reduced to thioether and thiol such as S-R under the action of rejuvenating agents.

Figure 17 shows that there is a close correlation between the softening point and the AI and CI. The softening point decreased as the aliphatic functional group index increased, for which the rate of decrease slowed, indicating that fatty substances were the only one of the influencing factors.

As shown in Figure 18, the recycled asphalt ductility has a good correlation with the AI and BI, which is basically

consistent with the increasing and decreasing curves of the CI and DI. The ductility of the recycled asphalt decreased as the BI, CI, and DI increased and improved as the AI increased.

The relationship between viscosity and the index of regenerated asphalt is shown in Figure 19. The CI and DI were positively correlated with the change in viscosity. This indicated that the increase in hydroxyl and sulfoxide functional groups of aged asphalt led to asphalt hardening and an increase in viscosity. Thus, preventing the formation

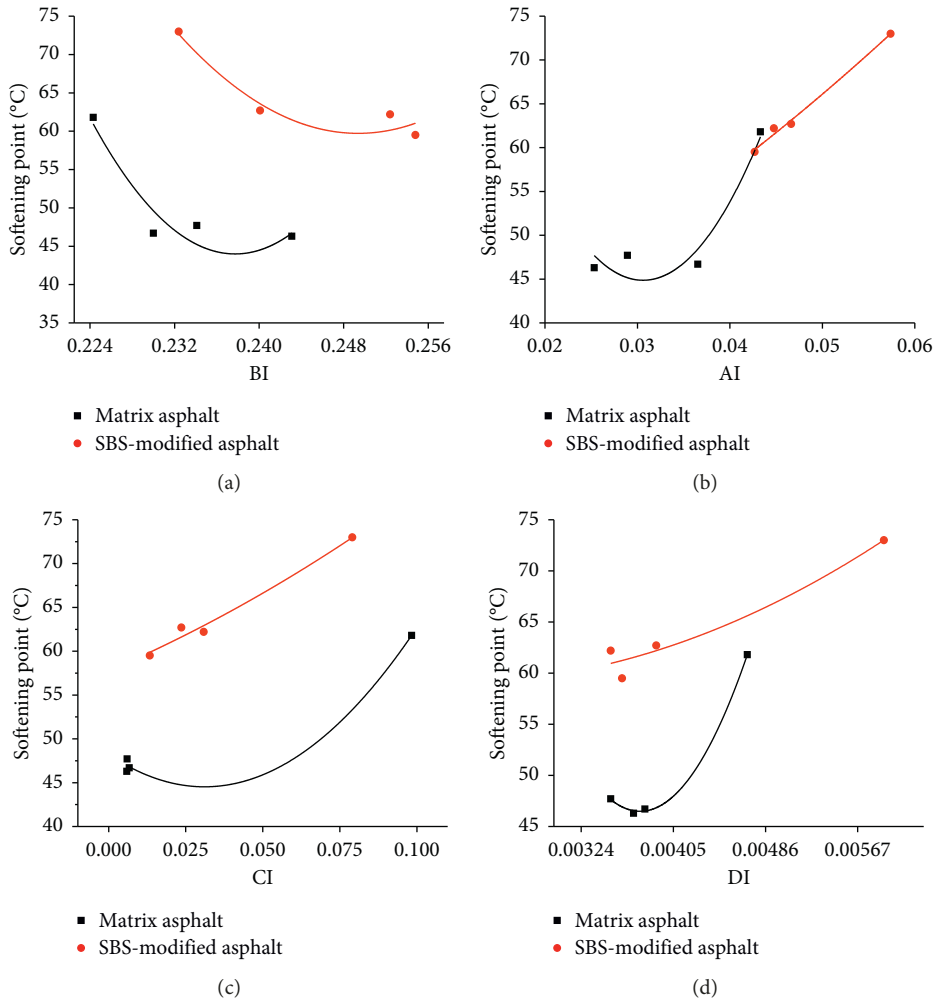


FIGURE 17: Relationships between the functional group indices and softening points.

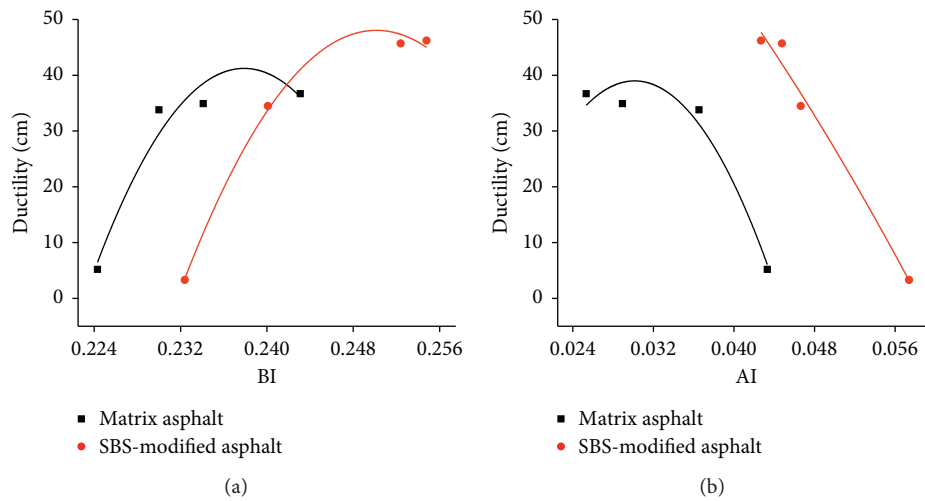


FIGURE 18: Continued.

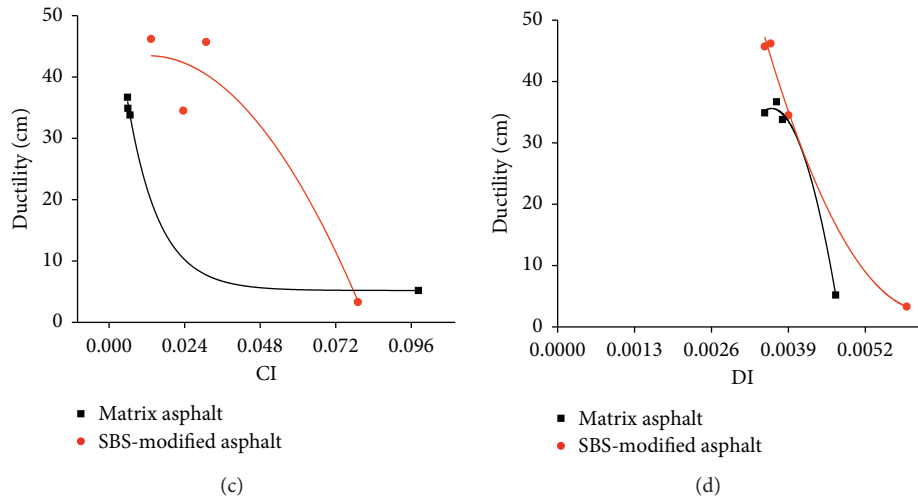


FIGURE 18: Relationships between the functional group indices and ductility.

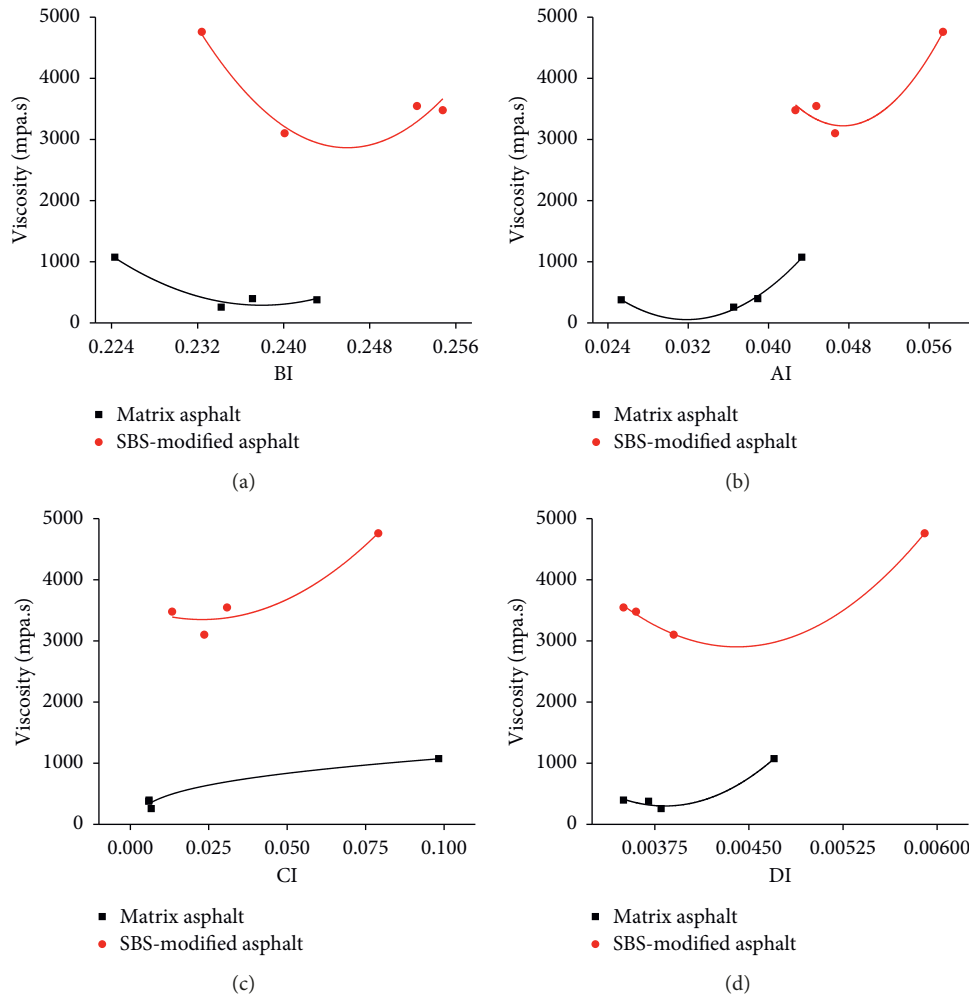


FIGURE 19: Relationships between various functional group indices and viscosity.

of these two functional groups in the process of asphalt aging could effectively guarantee a viscosity change, which provides a direction for future research of antiaging agents.

From the above analysis, it is observed that the long-chain alkyl decreases after aging of the asphalt. This is because the long chain breaks under the action of environmental factors, and the resulting free radicals are easily oxidized. The free radicals combine with oxygen to form various types of functional groups at the breaking points. The free radicals could combine with free sulfur to form sulfoxides under the action of oxygen. The alkane at the break combines with elemental oxygen in the air to form a carbonyl-containing aldehyde and a ketone-like substance. After the long chain of the benzene ring is cleaved, the hydrogen atom in the external group is easily substituted by a macromolecule to form a benzene ring substituent. After the asphalt is recycled, the added light components replenish the long-chain alkyl group and inhibit the formation of free radicals; the macromolecular benzene ring substituents are cleaved and replaced by hydrogen atoms, which reduces the content of aromatic compounds. The C=O and S=O bonds generated by the aging process are reduced to the C=C bond, S-R bond, etc. Thus, the molecular weight is reduced. The recycling process is the reverse process of asphalt aging, and components of rejuvenating agents have important roles in asphalt recycling.

#### 4. Conclusions

- (1) Compared to rejuvenating agents A and B, the penetration, softening point, viscosity, and ductility of the recycled asphalt with the rejuvenating agent CA could be recycled significantly, with performances close to those of the original asphalt.
- (2) The DSR tests showed that the compound shear modulus ( $G^*$ ), the phase angle ( $\delta$ ), and the rutting factor ( $G^*/\sin \delta$ ) after recycling were close to those of the original asphalt and that the recycled asphalt had excellent rheological properties after the addition of the rejuvenating agent CA.
- (3) The permeability performance of the rejuvenating agent could be evaluated by the penetration and improved softening point methods. Using these two methods, the rejuvenating agent CA was proved to be highly permeable.
- (4) Fourier transform infrared spectroscopy showed that the matrix asphalt experienced oxygen absorption and dehydrogenation during the aging process. The aging of SBS-modified asphalt was the result of dual aging of the matrix asphalt and SBS-modified components. After incorporating rejuvenating agents, the components were supplemented. Rejuvenating agents CA and A had similar effects on the recycling of the matrix asphalt. The rejuvenating agent CA had an inhibitory effect on the aging of SBS-modified asphalt, and its recycling capacity was better than that of the rejuvenating agent A for the aged SBS-modified asphalt.

#### Data Availability

Because the data in this paper are still a project of the Fundamental Research Funds for the Central Universities of China, the data need to be used in the follow-up study of this project. So all the data (figures and tables) used to support the findings of this study are supplied by the corresponding author under license and cannot be made freely available. Requests for access to these data should be made to Yanjuan Tian, Key Laboratory for Special Area Highway Engineering of Ministry of Education, Chang'an University, Middle Section of South Second Ring Road, 710064, Xi'an, Shaanxi, China (Tel: +86-298-233-4846; email: tianyj@chd.edu.cn).

#### Conflicts of Interest

The authors declare no conflicts of interest.

#### Acknowledgments

This research was sponsored by the Fundamental Research Funds for the Central Universities (Grant No. 310821163502), the Transportation Department of Shandong Province (Grant Nos. Lujiaokeyi [2017] 28 and 2013A01-01), the Xixian New District Management Committee of Shaanxi Province (Grant No. 2017 44), and the Science and Technology Bureau of Pingdingshan of China (Grant No. 2018610002000604). We express our gratitude to Mr. Hongyin Li for his support to this paper and many suggestions and help in the writing process.

#### References

- [1] M. A. Farooq, M. S. Mir, and A. Sharma, "Laboratory study on use of RAP in WMA pavements using rejuvenator," *Construction and Building Materials*, vol. 168, pp. 61–72, 2018.
- [2] Z. Feng, J. Yu, L. Xue, and Y. Sun, "Rheological and aging properties of ultraviolet absorber/styrene-butadiene-styrene-modified bitumens," *Journal of Applied Polymer Science*, vol. 128, no. 4, pp. 2571–2577, 2013.
- [3] A. Ongel and M. Hugener, "Impact of rejuvenators on aging properties of bitumen," *Construction and Building Materials*, vol. 94, pp. 467–474, 2015.
- [4] F. Xiao, S. Yao, J. Wang, X. Li, and S. Amirkhanian, "A literature review on cold recycling technology of asphalt pavement," *Construction and Building Materials*, vol. 180, pp. 579–604, 2018.
- [5] S. H. Carpenter and J. R. Wolosick, "Modifier influence in the characterization of hot-mix recycled materials," *Transportation Research Record*, vol. 777, pp. 15–22, 1980.
- [6] E. L. Cussler, *Diffusion-Mass Transfer in Fluid System*, Cambridge University Press, London, UK, 1997.
- [7] R. Karlsson and U. Isacson, "Application of FTIR-ATR to characterization of bitumen rejuvenator diffusion," *Journal of Materials in Civil Engineering*, vol. 15, no. 2, pp. 157–165, 2003.
- [8] F. Yu and N. Zheng, "Study on the diffusion of regenerant and asphalt," *Journal of China & Foreign Highway*, vol. 29, no. 5, pp. 229–232, 2009.
- [9] R. Karlsson and U. Isacson, "Laboratory studies of diffusion in bitumen using markers," *Journal of Materials Science*, vol. 38, no. 13, pp. 2835–2844, 2003.

- [10] F. Wang, Y. Wang, and Q. Zhang, "Study on regeneration effect and diffusion performance of asphalt regenerant," *Petrochemical Technology & Application*, vol. 30, no. 1, pp. 13–18, 2012.
- [11] L. Sun, Y. Wang, and Y. Zhang, "Aging mechanism and effective recycling ratio of SBS modified asphalt," *Construction and Building Materials*, vol. 70, pp. 26–35, 2014.
- [12] T. Ma, X. Huang, Y. Zhao, and Y. Zhang, "Evaluation of the diffusion and distribution of the rejuvenator for hot asphalt recycling," *Construction and Building Materials*, vol. 98, pp. 530–536, 2015.
- [13] Y. Zhang, "Effect of regenerant on road performance of high proportion RAP thermal recycled asphalt mixture," *Highways & Automotive Applications*, vol. 2, pp. 118–121, 2017, in Chinese.
- [14] L. Ran, Z. He, and Q. Cao, "Performance research of regenerative agent based on SBS-modified asphalt," *Journal of Building Materials*, vol. 18, no. 4, pp. 578–583, 2015.
- [15] L. Li, M. Zhang, and W. Qi, "Regeneration of aged SBS modified asphalt and its mechanism analysis," *Journal of Chang'an University (Natural Science Edition)*, vol. 37, no. 3, pp. 1–8, 2017.
- [16] M. Xu, J. Yi, D. Feng, and Y. Huang, "Diffusion characteristics of asphalt rejuvenators based on molecular dynamics simulation," *International Journal of Pavement Engineering*, vol. 20, no. 5, pp. 615–627, 2019.
- [17] E. Mohamed, R. Christopher Williams, and E. W. Cochran, "Thermal and cold flow properties of bio-derived rejuvenators and their impact on the properties of rejuvenated asphalt binders," *Thermochimica Acta*, vol. 671, pp. 48–53, 2019.
- [18] R. Zhang, Z. You, H. Wang, M. Ye, Y. K. Yap, and C. Si, "The impact of bio-oil as rejuvenator for aged asphalt binder," *Construction and Building Materials*, vol. 196, pp. 134–143, 2019.
- [19] H. F. Haghshenas, K. Yong-Rak, M. D. Morton, S. Thomas, K. Mahdih, and D. F. Haghshenas, "Effect of softening additives on the moisture susceptibility of recycled bituminous materials using chemical-mechanical-imaging methods," *Journal of Materials in Civil Engineering*, vol. 30, no. 9, article 04018207, 2018.
- [20] P. Caputo, V. Loise, A. Crispini, C. Sangiorgi, F. Scarpelli, and C. Oliviero Rossi, "The efficiency of bitumen rejuvenator investigated through Powder X-ray Diffraction (PXRD) analysis and T2-NMR spectroscopy," *Colloids and Surfaces A: Physicochemical and Engineering Aspects*, vol. 571, pp. 50–54, 2019.
- [21] Ministry of Transport, *Standard Test Methods of Bitumen and Bituminous Mixtures for Highway Engineering (JTG E20-2011)*, Ministry of Transport, Beijing, China, 2011.
- [22] ASTM D2872-19, *Standard Test Method for Effect of Heat and Air on a Moving Film of Asphalt (Rolling Thin-Film Oven Test)*, ASTM International, West Conshohocken, PA, USA, 2019, <http://www.astm.org>.
- [23] S.-C. Huang, M. Tia, and B. E. Ruth, "Laboratory aging methods for simulation of field aging of asphalts," *Journal of Materials in Civil Engineering*, vol. 8, no. 3, pp. 147–152, 1996.
- [24] P. Li, *Study on the Aging Behavior and Mechanism of Paving Asphalts*, Chang'an University, Xi'an, China, 2007.
- [25] C. Chen, *Development and Application Technology of Asphalt Pavement Rejuvenating Agent*, Chang'an University, Xi'an, China, 2016.
- [26] Ministry of Transport, *Technical Specifications for Construction of Highway Asphalt Pavements (JTG F40-2004)*, Ministry of Transport, Beijing, China, 2004.
- [27] J. Lamontagne, P. Dumas, V. Mouillet, and J. Kister, "Comparison by fourier transform infrared (FTIR) spectroscopy of different ageing techniques: application to road bitumens," *Fuel*, vol. 80, no. 4, pp. 483–488, 2001.
- [28] F. Zhang, J. Yu, and J. Han, "Effects of thermal oxidative ageing on dynamic viscosity, TG/DTG, DTA and FTIR of SBS- and SBS/sulfur-modified asphalts," *Construction and Building Materials*, vol. 25, no. 1, pp. 129–137, 2011.
- [29] X. Hou, S. Lv, Z. Chen, and F. Xiao, "Applications of fourier transform infrared spectroscopy technologies on asphalt materials," *Measurement*, vol. 121, pp. 304–316, 2018.
- [30] P. Cong, P. Xu, and M. Xing, "Experiment and study on compaction characteristics of warm asphalt mixture," *Highway*, vol. 5, no. 3, pp. 147–151, 2013, in Chinese.
- [31] Y. Zhao, F. Gu, and X. Huang, "Analysis on SBS modified asphalt aging characterization based on fourier transform infrared spectroscopy," *Journal of Building Materials*, vol. 14, no. 5, pp. 620–623, 2011.
- [32] Thermo Fisher Nicolet, *OMNIC Version 8.2 (Computer Software)*, Thermo Fisher Nicolet, Madison, WI, USA, 1999.

